Photodissociation of Sulfur Dioxide: The $\tilde{E}$ State Revisited

K. L. Knappenberger, Jr. and A. W. Castleman, Jr.*
Departments of Chemistry and Physics, The Pennsylvania State University, University Park, Pennsylvania 16802

Received: June 25, 2003

The pump−probe technique has been employed to study the photodissociation processes of sulfur dioxide (SO_2). The SO_2^+ transient has been fit to a biexponential with decay times of 230 ± 9 fs and 8 ± 4 ps. The growth of $^{32}SO^+$ was determined to be 225 ± 10 fs with a decay of 373 ± 27 fs. The response of the isotope $^{34}SO_2^+$ was also fit to a biexponential decay with lifetimes of 195 ± 14 fs and 4 ± 1 ps. The decay of $^{34}SO^+$ was fit to 381 ± 30 fs. The results display that an inverse kinetic isotope effect is operative during dissociation of SO_2 through the $\tilde{E}$ state.

Introduction

Many of the sulfur-containing molecules present in the atmosphere are introduced initially as sulfur dioxide through the combustion of fossil fuels as well as the natural emission of volcanic activity. Sulfur dioxide is readily oxidized in the atmosphere by chemical reaction or photolysis. Once oxidized, SO_2 may undergo a series of reactions ultimately leading to the formation of acid rain. The significance of these processes has stimulated research by our group[1−3] and others[4−8] in an effort to understand photochemical properties of sulfur dioxide when irradiated with UV photons. Sulfur dioxide has also been detected in the atmospheres of Venus and Jupiter's Io,[9] indicating it may be significant to astrophysical processes as well. Additionally, the question of isotopic influence over the photodissociation has been raised by a survey of geologic records.[10] Investigation of the fundamental dissociation processes of SO_2 is necessary to discern the molecule's role in the above issues.

The $\tilde{E}$ state was observed by Vušković and Trajmar[11] during electron impact excitation and assigned to the region consisting of a band of states at approximately 8 eV. An early report of the photochemistry SO_2 near the $\tilde{E}$ state by Lalo and Vermeil[4,5] using one photon excitation at 147 nm (∼8.5 eV) concluded two dissociation products are observable, SO + O and S + O_2. Effenhauser et al.[6] employed photofragment translational spectroscopy and published a quantitative report of the decay fraction obtained when photodissociation is initiated with two photons at 308 nm. The primary dissociation products are assigned to SO ($X^3\Sigma^-$) and SO ($a^1\Delta$).

Zhong et al.[1] studied the metastable decay of sulfur dioxide and sulfur dioxide−water binary cluster systems and reported the core structure of the cluster cations after excitation of the sulfur dioxide chromophore. Information regarding the influence clustering has on the SO_2 chromophore was extended by Hurley et al.,[3] who determined the primary dissociation process of the $C(2^1A')$ state. Dynamics of the $\tilde{E}$ state were reported previously by our group,[2] where the formation of sulfur monoxide was observed. The SO_2 transient was fit to an exponential decay of 271 ± 8 fs, in good agreement with the growth of the product SO. However, meaningful fits were not obtained for all dissociation fragments and the role of an isotope effect was not addressed.

Current research regarding sulfur dioxide cluster systems has led us to revisit the dynamics of the monomer. In this article we present the results of two multiphoton processes. By employing the pump−probe technique, we populate an excited state by the absorption of 312 nm photons and may access either the $\tilde{A}$ ($^1B_1$) state through the absorption of one photon or the $\tilde{E}$ state by the absorption of two pump photons.[11,12] By adjusting the delay of the 612 nm ionizing (probe) pulse, we record the evolution of the respective excited states. Pump−probe scans are extended to longer delay times and power studies are employed to elucidate the contribution of both states to the transient response. The technique is also applied to $^{34}SO_2$ and our interpretation is presented.

Experimental Section

Sulfur dioxide is introduced to the laser interaction region by the nascent expansion of sulfur dioxide vapor through a pulsed valve. The molecular beam is collimated by a skimmer before entering the expansion region. The extent of clustering can be controlled by adjusting the amount of time the pulsed valve is open.

Upon ionization, the distribution of the molecular beam is detected with a reflectron time-of-flight mass spectrometer. The mass spectrometer consists of several components,[13,14] an acceleration region, two field-free drift regions, a reflectron, and a pair of microchannel plate (MCP) detectors. The MCP plates are coupled to a digital oscilloscope (Agilent Technologies 54820A) which is then coupled to a PC for data analysis.

Sulfur dioxide is ionized via the resonant absorption of photons generated by a fs laser system which has been described in detail elsewhere.[15] Briefly, fs pulses are the output of a colliding pulse mode-locked ring dye laser (CPM). Amplification is achieved in four stages using a six-pass bowtie amplifier followed by three successive Bethune cells. Amplification is achieved in all four stages via transverse pumping with thesecond harmonic of a 10-Hz Nd:YAG laser (Spectra Physics GCR-4). After amplification, the recompressed pulse has a duration of <150 fs as determined by autocorrelation and is centered at 624 nm.

The results reported here are obtained via a two-color pump−probe experiment. Ultraviolet radiation, centered at 312 nm, is achieved by frequency doubling of the fundamental by focusing through a β-barium borate (BBO) crystal. The fundamental

* Author to whom correspondence may be addressed. E-mail: awc@psu.edu.

10.1021/jp030786y CCC: $27.50
Published on Web 12/10/2003

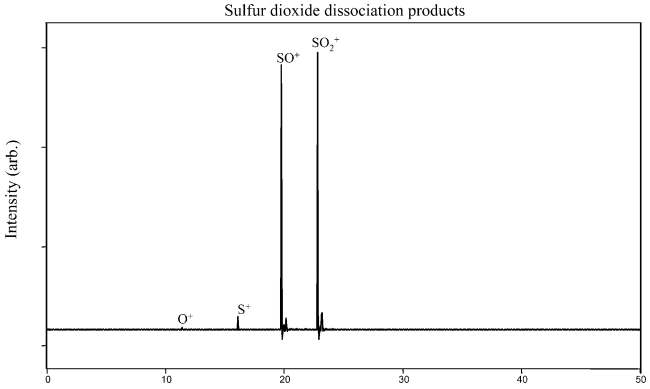

Figure 1. A truncated time-of-flight spectrum showing a typical mass spectrum of sulfur dioxide dissociation products.

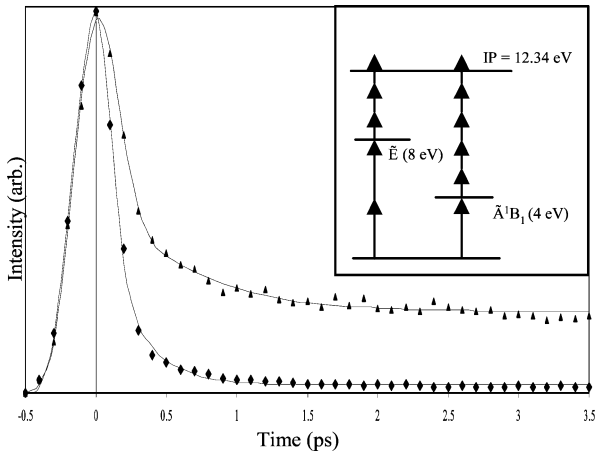

Figure 2. Comparison of SO_2 transient under conditions of high probe power (25 mW) and low probe power (13 mW) represented by triangles and dots, respectively. The inset is a schematic of the energy levels believed to be accessed in each configuration.

photons not converted to the second harmonic are harvested and used as the probe pulse. The generated UV light traverses a movable delay stage so that the differences in optical path length can be employed for dynamic studies. It should be noted that experimental conditions are set such that signal is not generated by either beam operating independently; rather, signal is observed only through the enhancement when both beams are present.

The fitting procedure we use employs a least-squares method and has been adopted from that described in detail by Zewail and co-workers.[17] The pump−probe data presented herein are fit to either single or biexponential decays of the form

$$S(t) = A\int_{-\infty}^{t} g(t)\exp\left(\frac{t-t_c}{\tau_1}\right)\mathrm{d}t \tag{1}$$

$$S(t) = A\int_{-\infty}^{t} g(t)\exp\left(\frac{t-t_c}{\tau_1}\right)\mathrm{d}t + B\int_{-\infty}^{t} g(t)\exp\left(\frac{t-t_c}{\tau_2}\right)\mathrm{d}t \tag{2}$$

$$g(t) = \frac{1}{\theta\pi^{1/2}}\exp -\left(\frac{t}{\sigma}\right)^2 \tag{3}$$

where the component $g(t)$ is a Guassian function included to account for the response generated by the correlation of the laser pulses. The term σ is related to the laser full width at half-maximum (fwhm) by the relation $\sigma = (\mathrm{fwhm}/\sqrt{1.6651})$. A and B are amplitude coefficients reflecting the contribution of each component to the total signal. The functions presented above are by their nature decay functions and intended to represent the disappearance of signal with time. When the transient contains a growth component, which represents the reappearance of signal, the corresponding amplitude coefficient will take on a negative value.

Results

Typical distributions of photodissociation products are shown in the mass spectrum of Figure 1, when sulfur dioxide is passed through the pulsed valve. Peaks corresponding to 16 and 32 amu are assigned as $^{16}O^+$ and $^{32}S^+$, respectively. The peak occurring at 32 amu was determined to be $^{32}S^+$ and not $^{16}O_2{}^+$ due to the isotopic abundance reflecting that of atomic sulfur.

Figure 2 depicts the temporal ion signal of $^{32}S^{16}O_2$ under two different pump−probe conditions. In the case of high probe power, the ion signal remains elevated at all times after zero delay for the duration of the scan, approximately 3.5 ps. The transient obtained while employing the lowest probe photon density of our studies is characterized by a very fast decay as the signal rapidly returns to baseline. We believe the inset of Figure 2 reflects the differences in the pump−probe transients. As the results of Vuśković et al.[11] demonstrate, our pump step can populate both the $\tilde{E}$ and $\tilde{A}^1B_1$ states. The scenario with high probe fluence enables ionization of SO_2 from either excited state, while the experiment employing low fluence only provides enough energy in the probe step to promote electrons populating the $\tilde{E}$ state to the ion state. The fast decay, which is the only feature present in the low fluence case, must reflect the dynamics of the excited $\tilde{E}$ state, while the elevated signal at long delay time is a result of the lower $\tilde{A}^1B_1$ state. Further, the $\tilde{A}^1B_1$ state is below the dissociation energy of sulfur dioxide, which was determined experimentally to be 5.3 ± 0.1 eV.[16] Therefore the long decay is a consequence of the population of a bound state.

To better resolve the characteristics of the temporal response, scans were conducted at longer delay times. As the wave packet evolves over a duration of 17 ps, the decay converges to the best fit as a biexponential decay. Only the values obtained for the decay rates are presented in the text; we report the standard deviation of each component in Table 1. The fast component, attributed to dissociation via the $\tilde{E}$ state, fits to a decay of 230 fs. The slow component, arising when ionization is promoted from the $\tilde{A}^1B_1$ state, fits to a decay of 8 ps. Additionally, at low probe power, the SO_2 transient fits only to a single-exponential decay with a lifetime of 231 fs, shown in Figure 6. As is evident in the mass spectrum of Figure 1, it is possible to distinguish between the sulfur isotopes. The inset of Figure 3 includes the lifetimes for the decay of both isotopes at long time delays. The temporal response of the $^{34}SO_2$ species was fit when the fast and slow components are fit to 195 fs and 4 ps, respectively, an indication of a possible isotope effect on the photodissociation process when compared to the decay of the $^{32}SO_2$ species. Again, the results of the study at low probe power only fit well to a single-exponential decay of 194 fs.

The $\tilde{E}$ state is expected to be responsible for the dissociation observed in our experiment, and it resides approximately 2.7 eV above the dissociation energy. Figure 4 reflects the temporal behavior of the dissociation products obtained when enough probe power is employed to detect ion signal at all delay times as well as the time constants fitting the dynamics. The species presented in Figure 4 are those containing ^{32}S. Focusing only on the fast component of the $^{32}SO_2$ transient, the decay is again fit to 230 fs. The SO transient exhibits a growth of 224 fs and a decay of 393 fs. The sulfur monoxide growth is in good

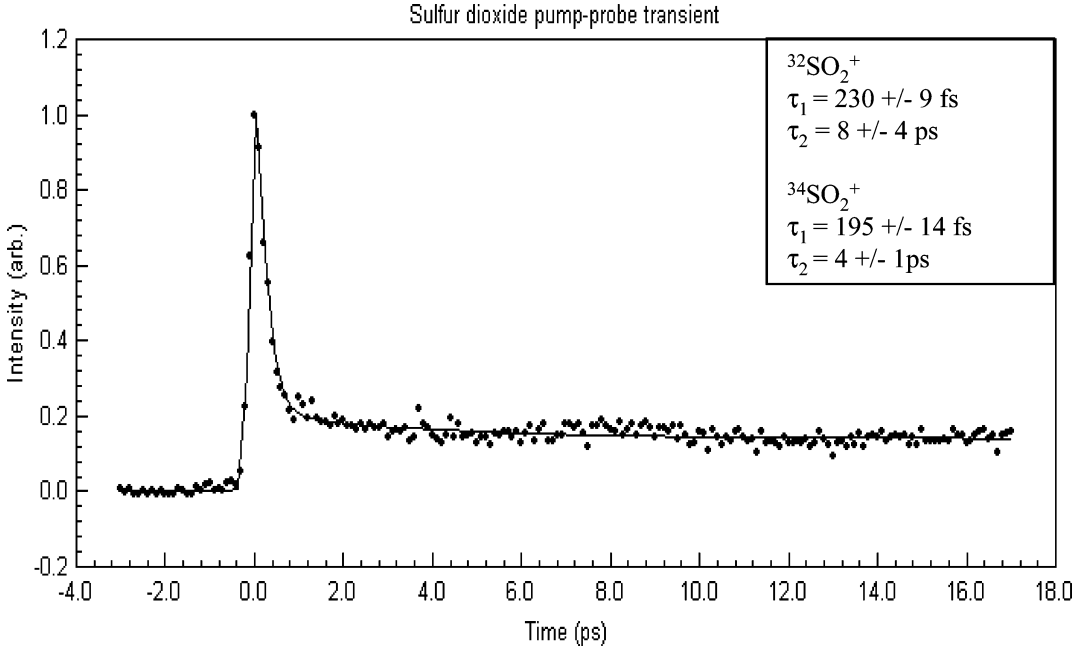

Figure 3. Temporal response of $^{32}SO_2^+$ at extended pump−probe delay times extending 17 ps after the zero overlap. The decay fits to a biexponential decay with the fast component decay at 230 ± 9 fs while the slow decay fits to 8.4 ± 3.7 ps. The response for $^{34}SO_2^+$ is similar except that the fast component decays in 195 ± 14 fs and the slow component decays in 3.8 ± 1.0 ps. The data were obtained by employing high fluence.

TABLE 1: Lifetime and Standard Deviation Obtained for Each Component When Employing Low (left) and High (right) Probe Laser Fluence

species	low fluence		high fluence	
$^{32}SO_2^+$	decay 1	231 ± 7fs	decay 1	230 ± 9 fs
	decay 2		decay 2	8 ± 4 ps
$^{34}SO_2^+$	decay 1	194 ± 8 fs	decay 1	195 ± 18 fs
	decay 2		decay 2	4 ± 1 ps
$^{32}SO^+$	growth	225 ± 10 fs	growth	224 ± 11 fs
	decay	373 ± 27 fs	decay	393 ± 32
$^{34}SO^+$	growth	187 ± 9 fs	growth	192 ± 6 fs
	decay	381 ± 30 fs	decay	399 ± 27 fs
$^{32}S^+$	growth	228 ± 5 fs	decay 1	212 ± 17 fs
	decay 2	385 ± 8 fs	decay 2	369 ± 20 fs
O^+	growth	ND	growth	229 ± 12 fs
	decay	ND	decay	791 ± 57 fs

agreement with the decay fit to sulfur dioxide indicating an A → B dissociation, where A is SO_2 and B is SO.

The remaining products represented in Figure 4 are those of ^{32}S and ^{16}O. The ^{32}S fragment is best fit to biexponential decay of 212 and 369 fs. The ^{16}O fragment, shown in Figure 4d, grows in at 229 fs and decays at 791 fs. The temporal behavior of the ^{32}S ion signal is characterized by a biexponential decay and the maximum signal intensity occurs when pump and probe pulses overlap at time zero. The decay times of the two components are in good agreement with the decay time obtained for the SO_2^+ and SO^+ signal indicating S^+ is formed as an ion state product of both species when high probe powers are employed. The ^{16}O response is characterized by a growth similar to the decay of SO_2 and a unique decay indicating it is a product of SO_2 predissociation.

Figure 5, similar in nature to Figure 4, reflects the dissociation process of the ^{34}S-containing species at the same laser probe power. The fast component of SO_2 is fit to 195 fs and is displayed in Figure 5a. The growth component of the mass 50 transient fits well to 192 fs while the decay fits to 399 fs, Figure 5b. The dynamical processes leading to the dissociation of the $^{34}SO_2$ species appear to mirror those of $^{32}SO_2$; however, they occur more rapidly.

The pump−probe response of ^{32}S-containing species is presented in Figure 6 when a low probe fluence is employed. The SO_2 response is fit to a single-exponential decay with a lifetime of 231 fs. Likewise, the growth of SO is fit to a rise time of 225 fs with a decay of 373 fs. The atomic sulfur ion displays features similar to the SO response with a growth and decay of 228 and 385 fs, respectively. Studies conducted at low probe power did not provide a sufficient number of photons to surmount the ionization threshold of molecular oxygen. The dynamics exhibited by those species containing the ^{34}S isotope are presented in Figure 7. The dissociation processes proceed in the same manner but are fit to different lifetimes. The $^{34}SO_2$ decays in 194 fs while the growth of ^{34}SO is fit to a rise and decay of 187 and 381 fs, respectively.

Discussion

The pump−probe transient of $^{34}SO_2$ observed in our experiment is fit to a biexponential decay, with the fast component decaying in 230 fs and resulting in predissociation to SO. The fast component is attributed to the $\tilde{E}$ state, which is located above the dissociation threshold. Furthermore, the best fit of the SO transient converges to a rise of 225 fs as the growth component of this species. The mechanisms associated with product formation are illustrated in the kinetic model shown in Figure 8. It should be noted that previous studies published by our group[2] concluded the decay of this state proceeded in 271 ± 8 fs, differing slightly from the present findings. We believe the differences in the fit can be attributed to the presence of the SO_2^+ ion signal obtained when electrons are ionized from the lower lying $\tilde{A}^1B_1$. Care has been taken in the present study to elucidate the influence the $\tilde{A}^1B_1$ state can have on the temporal SO_2^+ signal. At short pump−probe delays, as reported earlier, the contribution of the lower state can increase the lifetime of a single-exponential decay. Employing probe power studies as well as extending the pump−probe scan to longer delay times has led us to determine that the ion signal is a reflection of two states with the lifetime of the $\tilde{E}$ state being 230 ± 9 fs and that of the $\tilde{A}^1B_1$ state being 8 ± 4 ps. As was described in the Experimental Section, the fitting function is comprised of a

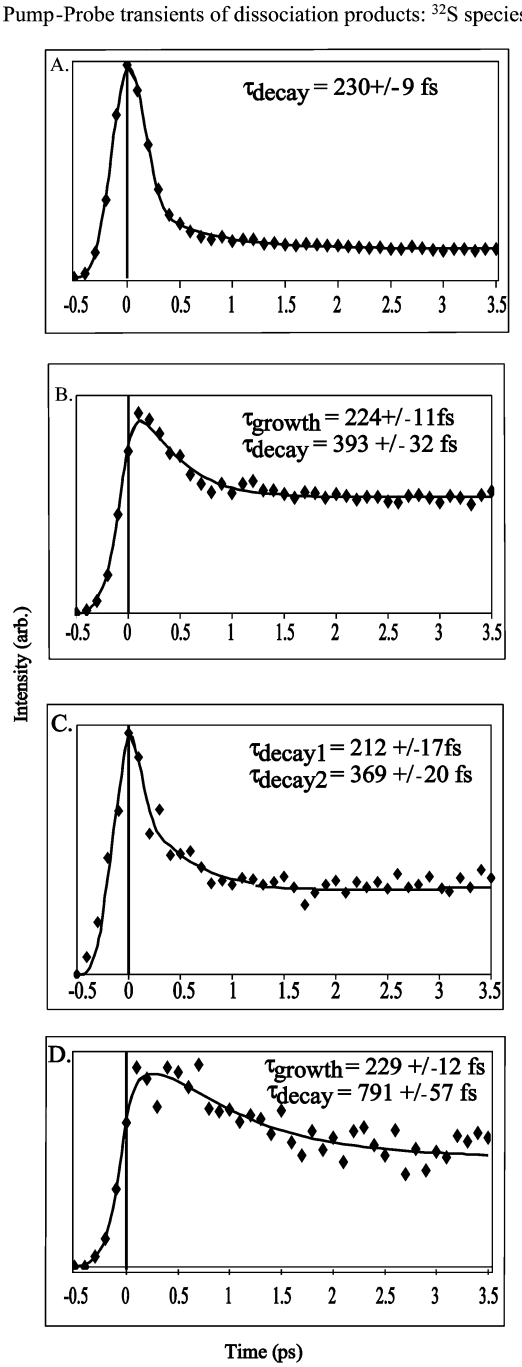

Figure 4. Photodissociation products of $^{32}SO_2^+$ after excitation to the $\tilde{E}$ state ionized with high probe power (25 mW). The dissociative channels are investigated over a period of 3.5 ps after the temporal overlap as the dissociative channel decays rapidly. The data were obtained by employing high fluence. The species include (A) $^{32}SO_2^+$, (B) $^{32}SO^+$, (C) S^+, and (D) O^+.

Gaussian component to convolute the laser pulse shape from the observed kinetics. It should be noted that our pulse width was measured by direct cross correlation. The value obtained from the DataFit fitting program is in very good agreement with this measured value.

Employing power studies is essential when studying multiphoton processes not only to determine the appropriate fit to each component but to ensure each component is attributed to the proper state. We first consider population of the $\tilde{A}^1B_1$ state by absorption of one 312-nm pump photon. Since this state is not predissociative, only ion-state products need to be considered. Ionization from the $\tilde{A}^1B_1$ state would require five photons

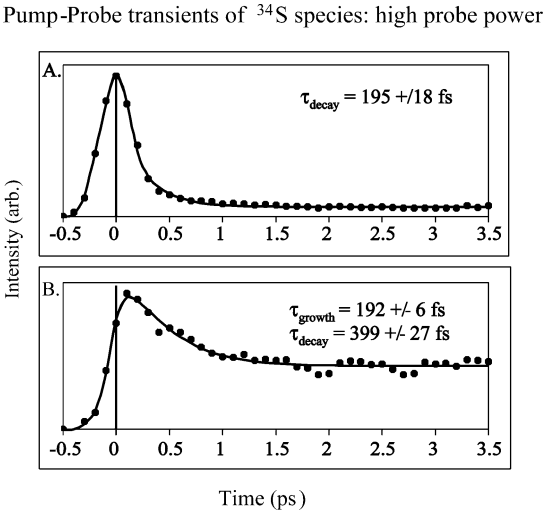

Figure 5. Photodissociation products of $^{34}SO_2^+$ after excitation to the $\tilde{E}$ state ionized with high probe power (25 mW). The dynamics are analogous to those of $^{32}SO_2^+$; however, the decay times are significantly shorter. The species include (A) $^{34}SO_2^+$ and (B) $^{34}SO^+$.

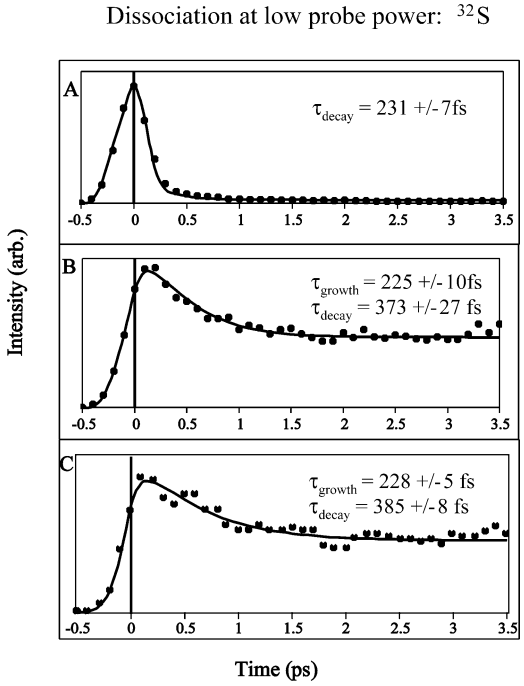

Figure 6. Photodissociation products of $^{32}SO_2^+$ after excitation to the $\tilde{E}$ state ionized with low probe power (13 mW). The species include (A) $^{32}SO_2^+$, (B) $^{32}SO^+$, and (C) $^{32}S^+$. Notice atomic oxygen is not ionized in the low-power study.

in the probe step and provide 1.55 eV over the ionization threshold. Thomas et al.[7] indicates 3.627 eV in excess of the ionization potential of SO_2 is necessary to induce ion state dissociation. Therefore, the only product resulting from ionization via the $\tilde{A}^1B_1$ state would be the SO_2 molecular ion.

The decay of the SO_2 isotopes were fit to either single or biexponential decays when employing low and high probe power, respectively. A Guassian function was incorporated to deconvolute the laser pulse shape. The transient of the SO species was fit by a series of rate equations in a consecutive reaction

$$A \xrightarrow[k_a]{} B \xrightarrow[k_b]{} C$$

Where A is SO_2, which decays to SO in the first step followed

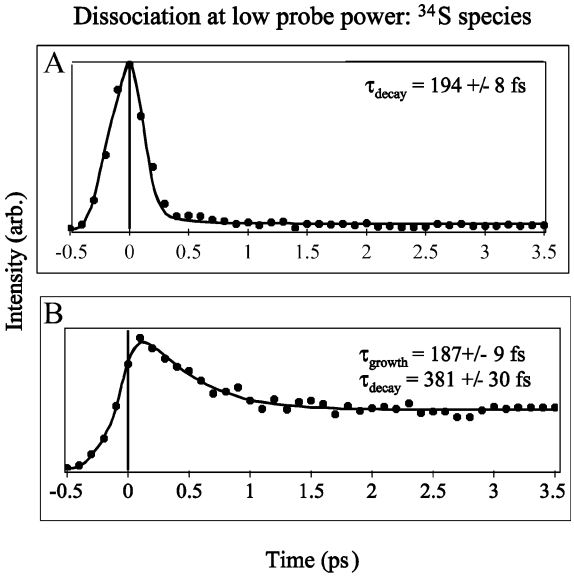

Figure 7. Photodissociation products of $^{34}SO_2^+$ after excitation to the $\tilde{E}$ state ionized with low probe power (13 mW). The species include (A)$^{34}SO_2^+$ and (B) $^{34}SO^+$.

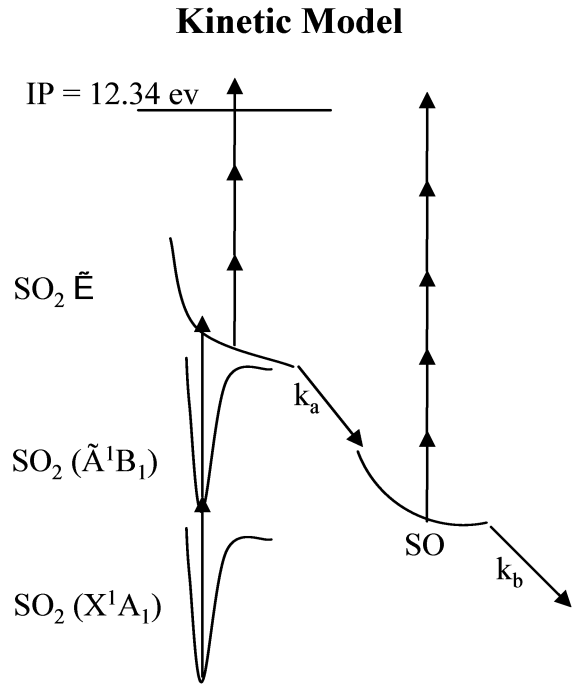

Figure 8. Kinetic model used to explain the dynamics observed as sulfur dioxide dissociates to form sulfur monoxide as well as the formation of S^+ and O^+ in the ion state.

by the decay of excited SO to a lower energy level. The rate constant reflecting the growth of SO is represented as k_a, and the subsequent decay of the excited product decays at a rate of k_b, shown schematically in the kinetic model of Figure 8. The rates are obtained from the inverse of the decay times reported in the results section.

The dissociation dynamics associated with the $\tilde{E}$ state are explained through interpretation of the results obtained from the best fits and comparison with the kinetic model of Figure 8. Absorption of two 312-nm photons by sulfur dioxide results in excitation to the $\tilde{E}$ state. Population of this state, which is coupled to a dissociative channel, leads to a rapid decay, 230 fs, as is reflected in the corresponding growth of sulfur monoxide, 225 fs. Interestingly, sulfur monoxide does not appear to exhibit significant enhancement at the zero overlap of the two laser pulses typically associated with strong field effects. Rather, the most intense ion signal occurs after the temporal overlap, indicating the sulfur monoxide signal is a result of the predissociation of sulfur dioxide. As was mentioned previously, absorption of as many as five probe photons appears to lead to ionization of SO_2 through the $\tilde{A}^1B_1$ state. Ionization through the $\tilde{E}$ state by absorption of up to five photons must also be considered. This scenario would provide 5.525 eV in excess of the SO_2 ionization potential. Referring to photodissociation studies on SO_2 ion states reported by Thomas et al.,[7] the ability to access levels of the SO_2 ion state 3.907 eV above the ionization potential would yield the sulfur atomic ion. It appears that under our conditions, we promote electrons from the $\tilde{E}$ state directly to a dissociative ion state producing S^+, and as a result the ion signal obtained in the high probe power case is due to formation of S^+ as an ion state product of both SO_2 and SO. The SO cations detected in our experiment are primarily a result of predissociation from the $\tilde{E}$ state, thus explaining the delayed maximum intensity of the SO temporal ion signal.

Lalo and Vermeil[4,5] reported results on the photolysis of SO_2 at 147 nm, and Effenhauser et al.[6] published two-photon dissociation of sulfur dioxide at 308 nm. Both groups indicated that SO was a likely dissociation product, while Effenhauser et al.[6] concluded that the likely products resulting from the absorption of two 308-nm photons by SO_2 would be

$$SO_2 + h\nu\ (2\ @\ 308\ \text{nm}) \rightarrow SO\ (X^3\Sigma^-) + O(^3P):1$$
$$\rightarrow SO\ (a^1\Delta) + O(^3P):2$$
$$\rightarrow SO\ (X^3\Sigma^-) + O(^1D):1$$

The above products are followed by their branching ratios. Furthermore, they noted that they could not discount the formation of the energetically possible SO ($b^1\Sigma^+$), although it was not observed in their experiment. It is anticipated that this state would be short-lived as it undergoes spontaneous emission as a relaxation mechanism. If dissociation of the SO_2 $\tilde{E}$ state produced the ground-state product, absorption of six probe photons would be required for ionization.[2,6] While this cannot be dismissed, we believe formation of an SO excited state is more likely. Ionization of SO ($^1\Delta$), or a product in a higher excited state, would only require absorption of five or less probe photons,[2,6] being more consistent with our interpretation of the SO_2 transient. The decay of the SO transient, τ_2 in Figure 5, is 393 fs, however measurable signal is present for the duration of the scan lasting 3.5 ps. Although the decay is fit to 393 fs, the excited population appears to relax to a bound state.

Wisniewski et al.[2] previously reported the decay of SO^+ to be that of a single exponential of 156 fs. The current investigation regarding the influence laser probe power has on the dissociation dynamics of SO_2 brings us to conclude the appropriate value of this decay is 390 fs. The previous study was conducted with pump photon intensities that generated SO_2 and SO ion signals even without a contribution from the probe.[18] Measures were taken in the present study to ensure that this was not the case. The pump-induced dissociation of the previous study may have complicated the temporal response, and the fit may not have solely reflected dissociation of the neutral state species.

The sulfur and oxygen atomic ions are formed in much less abundance than the molecular ions. The decay of sulfur is fit to a biexponential with decay times of 212 and 369 fs with maximum intensity at the temporal zero when high probe power is employed. This agrees with our interpretation of ionization

TABLE 2: Required Energy (ΔE) and Number of Photons Necessary To Ionize Parent and Products Studied in This Experiment

product	parent	ΔE (eV)	no. of photons
SO_2^+	SO_2 ($\tilde{E}$)	4.34	3
SO_2^+	SO_2 ($\tilde{A}$ 1B1)	8.43	5
SO^+	SO_2 ($\tilde{E}$)	7.96	4
SO^+	SO (x)	10.29	6
SO^+	SO ($^1\Delta$)	9.54	5
$\tilde{S}^+$	SO_2 ($\tilde{E}$)	8.24	5
S^+	S	10.36	6
O^+	O	13.62	7
O^+	O_2	18.69	10

from the SO_2 $\tilde{E}$ state, that S^+ is a directly formed ion state product. The slower decay time is similar to that obtained for SO^+, suggesting it is also an ion state product of sulfur monoxide. The ion signal of atomic oxygen is fit to a growth of 229 fs and a decay of 791 fs and closely resembles the growth behavior of the sulfur monoxide transient, indicating it arises from processes associated with the predissociation of sulfur dioxide. It appears that one of the dissociation products of sulfur dioxide is an excited oxygen atom, which decays in 791 fs and remains present in a bound state at long time delays. As is evident by the mass spectrum of Figure 1, the intensity of the atomic oxygen ion signal is significantly less than the rest of the dissociation products, indicating its formation is not a primary pathway. The energy required for the formation of the various fragments is shown in Table 2. The values presented indicate that formation of O^+ is the most energetically expensive process.

The kinetic model described above can also be applied to those species containing the ^{34}S isotope. The interpretation is straightforward from the ^{32}S species as $^{34}SO_2$ undergoes both multiphoton processes. However, the time constants fit to these species are somewhat different. The lower-lying state decays after 4 ps while the S−O bond cleavage resulting from dissociation along the $\tilde{E}$ state, occurs in only 195 fs. Similarly, the SO transient growth is approximately 192 fs and decays in only 399 fs. The results indicate a kinetic isotope effect is operative when comparing the excited dynamics of the $^{32}SO_2$ and $^{34}SO_2$ isotopic species. Considering SO_2, where we let k_{32} and k_{34} represent the decay rates of the $^{32}SO_2$ and $^{34}SO_2$ molecules, respectively, $k_{32} = 4.34$ ps^{-1} (230 fs) and $k_{34} = 5.12$ ps^{-1} (195 fs). The ratio $k_{32}/k_{34} = 0.848$, indicating a small inverse kinetic isotope effect. This effect was found to be reproducible. Kinetic isotope effects have been observed in a few pump−probe experiments; relevant examples can be found in the literature.[19−21] While a complete review is not appropriate here, we do find it worthwhile to mention the report of Radloff and co-workers regarding the dissociation of CS_2.[20] It was determined that $C^{32}S^{34}S$ dissociated in 170 fs as compared to $C^{32}S_2$ which dissociated in 210 fs, indicating an inverse kinetic isotope effect similar to that measured by us and reported herein.

Our experiments provide information regarding the dissociation of SO_2 to SO via the $\tilde{E}$ state. A more detailed understanding requires an accurate description of the potential energy surface, which unfortunately is lacking for the state addressed in this study. A monograph by Van Hook[22] discussed the sensitive isotopic dependencies often displayed by bending modes resulting in a significant contribution to kinetic isotope effects. High level ab initio studies of SO_2 dissociation through the C ($^1B_1$) state, which is slightly lower in energy than the $\tilde{E}$ state, were reported. The results showed that the C ($^1B_1$) state couples to a bending channel that proceeds as the bond angle increases from the ground-state equilibrium structure of 119.5° to a linear configuration at 180°, at which point dissociation occurs.[23] The results of our experiments are consistent with the suggestion that a bending mode and its crossing with a repulsive state may be responsible for the predissociation observed for the SO_2 isotopes.

Conclusions

Sulfur dioxide is shown to dissociate via the excited $\tilde{E}$ state resulting in the cleavage of an S−O bond to form sulfur monoxide in 230 ± 9 fs. Photodissociation to SO is believed to form the SO excited-state product. It has also been demonstrated that the $\tilde{A}^1B_1$ state of SO_2 is accessed, whose long lifetime results in the ion signal at long delay time. The pump−probe experiment has been used to elucidate the photochemical properties of molecules containing sulfur isotopes and conclude that an inverse kinetic isotope effect is present for sulfur dioxide. The results indicate the influence of the isotope is significant in determining the decay rate of the photodissociation process. The results glean information toward a better understanding of relevant dissociation processes occurring in the photochemistry of SO_2. This preliminary body will be extended to the study of clusters, which provide a significant model for the understanding of the mechanism associated with the heterogeneous chemistry of sulfur oxides.

Acknowledgment. Financial support by the Department of Energy, Grant No. 428.21-480F, is gratefully acknowledged.

References and Notes

(1) Zhong, Q.; Hurley, S. M.; Castleman, A. W., Jr. *Int. J. Mass. Spectrom. Ion. Processes* **1999**, *185/186/187*, 905.
(2) Wisniewski, E. S.; Castleman, A. W., Jr. *J. Phys. Chem. A* **2002**, *106*, 10843.
(3) Hurley, S. M.; Dermota, T. E.; Hydutsky, D. P.; Castleman, A. W., Jr. *J. Phys. Chem. A* **2003**, *107*, 3497.
(4) Lalo, C.; Vermeil, C. *J. Photochem.* **1973**, *1*, 321.
(5) Lalo, C.; Vermeil, C. *J. Photochem.* **1975**, *3*, 441.
(6) Effenhauser, C. S.; Felder, P.; Huber, J. R. *Chem. Phys.* **1990**, *142*, 311.
(7) Thomas, T. F.; Dale, F.; Paulson, J. F. *J. Chem. Phys.* **1986**, *84*, 1215.
(8) Sato, T.; Kinugawa, T.; Arikawa, T.; Kawasaki, M. *Chem. Phys.* **1992**, *165*, 173.
(9) Strobel, D. F.; Wolven, B. C. *Astrophys. Space Sci.* **2001**, *277*, 271.
(10) Pavlov, A. A.; Kasting, J. F. *Astrobiology* **2002**, *2*, 27.
(11) Vuśković, L.; Trajmar, S. *J. Chem. Phys.* **1982**, *77*, 5436.
(12) Huber, K. P.; Herzberg, G. *Molecular Spectra and Molecular Structure: Constants of Diatomic Molecules*; Van Nostrand Reinhold Company: New York, 1979.
(13) Mamyrin, B. A.; Karateav, V. I.; Shmikk, D. V.; Zagulin, V. A. *Sov. Phys. JETP* **1973**, *37*, 45.
(14) Wiley, W. C.; McLaren, I. H. *Rev. Sci. Instrum.* **1955**, *26*, 1150.
(15) Purnell, J.; Wei, S. A.; Buzza, S. A.; Castleman, A. W., Jr. *J. Phys. Chem.* **1993**, *97*, 12530.
(16) Jursic, B. S. *THEOCHEM* **1999**, *467*, 187.
(17) Pederson, S.; Zewail, A. H. *Mol. Phys.* **1996**, *89*, 1455.
(18) Wisniewski, E. S. Personal communication.
(19) Owrutsky, J. C.; Baronavski, A. P. *J. Chem. Phys.* **1999**, *110*, 11206.
(20) Farmanara, P.; Stert, V.; Radloff, W. *J. Chem. Phys.* **1999**, *111*, 5338.
(21) Fiebig, T.; Wan, C.; Zewail, A. H. *Chem. Phys. Chem.* **2002**, *3*, 781.
(22) Van Hook, W. A. In *Isotope Effects in Chemical Reactions*; Collins, C. J., Bowman, N. S., Eds.; ACS Monograph 167; American Chemical Society: New York, 1970; pp 1−84.
(23) Kamiya, K.; Matsui, H. *Bull. Chem. Soc. Jpn.* **1991**, *64*, 2792.